Low-momentum classical mechanics with effective quantum potentials

F. Haas*
Unidade de Exatas e Tecnológicas, Universidade do Vale do Rio dos Sinos—UNISINOS, Av. Unisinos, 950, 93022-000 São Leopoldo, RS, Brazil

(Received 7 February 2005; revised manuscript received 15 March 2005; published 24 June 2005)

A recently introduced effective quantum potential theory is studied in a low-momentum region of phase space. This low-momentum approximation is used to show that the effective quantum potential induces a space-dependent mass and a smoothed potential, both of them constructed from the classical potential. The exact solution of the approximated theory in one spatial dimension is found. The concept of effective transmission and reflection coefficients for effective quantum potentials is proposed and discussed in comparison to an analogous quantum statistical mixture problem. The results are applied to the case of a square barrier.

DOI: 10.1103/PhysRevB.71.235111 PACS number(s): 03.65.Xp, 03.65.Nk, 05.60.Gg

I. INTRODUCTION

In nano-MOSFETs, resonant tunneling diodes and other microelectronic devices, quantum effects are known to play a significant role.[1] Recently, there have been some efforts to create models incorporating quantum effects for microelectronic devices in a less expensive way than, for instance, the Wigner-Poisson model.[2] One of these simplified approaches is based on effective quantum potentials.[3] The aim of effective quantum potential methods is to replace the quantum transport equations by a classical transport theory with a modified potential, reproducing to some extent the essential quantum effects of the problem. To be faithful, an effective quantum potential theory must have similar or lower computational complexity than the quantum transport equations. In addition, it must reduce to classical transport theory for a vanishing Planck's constant. Apart from more pragmatic purposes, effective quantum potentials have also attracted attention as an attempt to return to phase-space and classical statistical mechanics. For a general introduction on the subject of effective potentials, the reader can see Refs. 4 and 5 and the references therein.

Recently,[5,6] an effective quantum potential has been proposed and applied[7] to model nano-MOSFETs of 25 nm. The advantage of this method over the previous ones is that it does not require the introduction of a fitting parameter to be adjusted at the beginning of the simulations. Indeed, for effective quantum potentials constructed from Gaussian smoothing of the classical potential, there has been some controversy about the correct value of the smoothing parameter. Specifically,[4,8,9] effective quantum potentials $V_{\mathrm{Gauss}}(q)$ obtained from Gaussian smoothing of the classical potential $V^C(q)$ according to

$$V_{\mathrm{Gauss}}(q) = \frac{1}{\sqrt{2\pi}\sigma} \int V^C(q+q') \exp\left(-\frac{q'^2}{2\sigma^2}\right) dq',$$

the smoothing parameter being σ. The smoothing parameter is related to the nonzero size of the electron wave packet, and its value changes in a decisive way the position and the value of the peak of charge density in simulations.[4] For some candidates for σ, see Ref. 4. In contrast, in this effective quantum potential method the size of the wave packet is determined by the particle's energy, with no need of adjustable parameters. The derivation of the effective potential comes from the fact that the Wigner-Bloch and quantum Boltzmann equations should have identical stationary solutions. The details on the derivation can be found in.[5,6]

The effective quantum potential introduced in Refs. 5 and 6 depends in a nontrivial way on momentum. This obscures its interpretation and the construction of analytical results. From the conceptual viewpoint, this is a disadvantage over methods based on Gaussian smoothing only, where the effective quantum potential is not momentum dependent. To circumvent these difficulties and to obtain a more profound understanding of this effective quantum potential, the present work proposes a low-momentum approximation, restricting to a low-momentum region of phase space. As will be seen, for these low-energy cases this effective potential amounts to the introduction of a space- dependent mass and of a smeared potential. For simplicity, we restrict to one-dimensional problems. In this case, the low-momentum approximation allows for the complete integrability of the equations of motion. From the exact solution of the dynamics we can get detailed information about the structure of the effective quantum potential theory.

One of the main objectives of effective quantum potentials is the description of tunneling over barriers using a classical language. Nevertheless, tunneling is a nonlocal phenomenon that probably cannot be exactly matched by local effective potential theories.[4] In addition, of course, it is somewhat misleading to talk about transmission coefficients and so on when using effective quantum potentials. Indeed, in this case we would have simply "tunneling" as a result of particles undergoing classical transport over the barrier. Nevertheless, it is interesting to consider, in detail, the transport of particles in our effective quantum model. For this purpose we consider here the specific case of a square barrier, introducing an effective transmission coefficient associated to the effective quantum potential. This effective transmission coefficient is analog to the traditional transmission coefficient of quantum mechanics, but has a different nature. We define it as the fraction of particles surpassing the barrier of the effective quantum potential, for a beam of particles going from the left and with equally spaced energies ranging from zero up to the height of the classical barrier. A similar defi-

nition is introduced for the effective reflection coefficient. Even if these effective coefficients are not strictly analog to the quantum ones, they are useful for a quantitative analysis of tunneling in effective quantum potential theories. In addition, we consider also the more realistic situation of an incoming beam of particles with a Gaussian probability distribution in momentum.

The work is organized as follows. In Sec. II, the explicit form of the effective quantum potential is introduced. The effective quantum potential is expanded considering small energies, leaving us with an approximated form characterized by a space-dependent mass and a smeared potential. In Sec. III, the exact solution for the classical mechanics associated to the approximated effective quantum potential is constructed. With the aid of the analytical results of Sec. II and III, in Sec. IV the case of a square barrier is analyzed in detail. In particular, we explicitly obtain the effective quantum potential and effective transmission and reflection coefficients. We compare these coefficients with the transmission and reflection coefficients found in the strictly quantum case. Section V is reserved for the conclusions.

II. CLASSICAL MECHANICS WITH EFFECTIVE QUANTUM POTENTIALS

Our effective quantum potential theory is described by

$$\dot{q} = \frac{\partial \varepsilon^{\text{eff}}}{\partial p}, \quad \dot{p} = -\frac{\partial \varepsilon^{\text{eff}}}{\partial q}, \tag{1}$$

where the effective Hamiltonian is

$$\varepsilon^{\text{eff}}(q,p) = \frac{p^2}{2m} + V^{\text{eff}}(q,p). \tag{2}$$

In Eq. (2), the effective quantum potential is not simply a Gaussian smoothing, being defined according to the recent works,[5,6]

$$V^{\text{eff}}(q,p) = \int \Gamma(q-q',p) V^C(q') dq', \tag{3}$$

where $V^C(q)$ is the classical potential and

$$\Gamma(q-q',p) = \frac{1}{2\pi} \int \frac{2m}{\beta\hbar pk} \sinh\left(\frac{\beta\hbar pk}{2m}\right) \times \exp\left[-\frac{\beta\hbar^2 k^2}{8m} + ik(q-q')\right] dk. \tag{4}$$

In Eq. (4), $\beta=(\kappa_B T)^{-1}$ as usual. Observe that the integral smoothing (3) reduces fluctuations, a welcomed result especially in the neighborhood of heterojunctions.

From (3) it follows that the effective quantum potential is momentum dependent. This fact renders the equations of motion difficult to solve, in general. However, the form of the integral (4) suggests an useful approximation. Indeed, let us restrict to small momenta

$$\beta\hbar pk/m \ll 1 \tag{5}$$

to expand the hyperbolic sine at (4). Of course, the approximation (5) has to be carefully justified since k is not fixed in the integral, so that, even for small p, the condition (5) may not be satisfied. However, the exponential in (4) is negligible for large k, provided

$$\beta\hbar^2 k^2/m \gg 1. \tag{6}$$

When the argument of the hyperbolic sine at (4) is not negligible, so that $\beta\hbar pk/m \approx 1$, Eq. (6) can be used to disregard higher-order terms provided

$$\beta p^2/m \ll 1. \tag{7}$$

Indeed, substituting $\hbar k \approx m/(\beta p)$ into (6), we get (7). For even large wave numbers, the approximation becomes still more accurate. In view of the above arguments, for not too large momenta, it is justifiable to expand the hyperbolic sine at (4) up to $O(\beta p^2/m)$. This gives

$$V^{\text{eff}}(q,p) = V(q) + \frac{1}{2}\left(\frac{1}{M(q)} - \frac{1}{m}\right)p^2 + O\left(\frac{\beta p^2}{m}\right)^2, \tag{8}$$

where

$$V(q) = \frac{1}{2\pi} \int dk dq' \exp\left[-\frac{\beta\hbar^2 k^2}{8m} + ik(q-q')\right] V^C(q'), \tag{9}$$

$$M^{-1}(q) = m^{-1} + \frac{\beta^2\hbar^2}{24\pi m^2} \int dk dq' k^2 \times \exp\left[-\frac{\beta\hbar^2 k^2}{8m} + ik(q-q')\right] V^C(q'). \tag{10}$$

Note that the expansion is to all orders of $\hbar$, the only restriction being to consider small momenta. Taking into account (8), we obtain the approximated effective quantum Hamiltonian

$$\varepsilon^{\text{eff}}_{\text{approx}} = \frac{p^2}{2M(q)} + V(q), \tag{11}$$

the Hamiltonian for a particle of position-dependent mass under a time- independent potential. Quantum corrections are present both in $V(q)$ and $M(q)$.

III. EXACT SOLUTION

Hamilton equations for $\varepsilon^{\text{eff}}_{\text{approx}}(q,p)$ read

$$\dot{q} = \frac{p}{M}, \quad \dot{p} = -\frac{dV}{dq} + \frac{1}{2M^2}\frac{dM}{dq}p^2. \tag{12}$$

Eliminating p and restricting to level sets of constant energy $\varepsilon^{\text{eff}}_{\text{approx}} = \varepsilon$, the result is

$$\ddot{q} = -\frac{1}{M}\frac{dV}{dq} + \frac{(V-\varepsilon)}{M^2}\frac{dM}{dq} \tag{13}$$

or

$$m\ddot{q} = -\frac{dV^Q(q)}{dq}, \tag{14}$$

with the potential

$$V^Q(q) = \frac{m}{M(q)}(V(q) - \varepsilon) + \varepsilon. \tag{15}$$

The interpretation of (14) is as follows. At least for low momenta, the effective quantum potential induces modifications of the original classical potential, so that the final result is classical motion under the potential (15). The exact solution for (14) then follows from elementary methods. For $\hbar \to 0$, we have $M \to m$ and $V \to V^C$, so that $V^Q \to V^C$ and the classical Newtonian equation is recovered. The addition of the irrelevant numerical constant ε at the end of (15) was just a matter of convenience to obtain the correct classical limit when $\hbar \to 0$.

The usefulness of the form (15) together with (9) and (10) is that it provides a clean way to observe the modifications produced by quantum effects in the effective quantum potential model. For a given classical potential, we have a recipe for constructing the potential V^Q and to study the corresponding completely integrable Newtonian equation. In particular, this strategy can be used to obtain conclusions about tunneling rates related to the smearing of the classical potential when replaced by the potential V^Q. This possibility will be explored in Sec. IV.

IV. TUNNELING

Consider a square potential barrier centered at $q=0$, height V_0, and width $2L$, given by

$$V^C = V_0[\theta(L+q) + \theta(L-q) - 1], \tag{16}$$

where θ is the unit step function. The potential (16) was chosen for its simplicity only; the specific choice of the form of the potential barrier does not affect, in a decisive way, the results. Using (9) and (10), we obtain

$$V = \frac{V_0}{2}\left[\operatorname{erf}\left(\frac{\sqrt{2m}(L+q)}{\sqrt{\beta\hbar^2}}\right) + \operatorname{erf}\left(\frac{\sqrt{2m}(L-q)}{\sqrt{\beta\hbar^2}}\right)\right], \tag{17}$$

$$M^{-1} = m^{-1} + \frac{2V_0}{3\hbar}\left(\frac{2\beta}{\pi m}\right)^{1/2}\exp\left(-\frac{2m}{\beta\hbar^2}(L^2+q^2)\right) \times \left[L\cosh\left(\frac{4mLq}{\beta\hbar^2}\right) - q\sinh\left(\frac{4mLq}{\beta\hbar^2}\right)\right], \tag{18}$$

where erf is the error function. The quantum potential V^Q then follows from (15).

Graphics of the space-dependent mass are shown in Fig. 1, with $m=1$, $L=1/2$, $V_0=1$, $\beta=1/8$, and two different values of $\hbar$, namely, $\hbar=10$ (full line) and $\hbar=30$ (dotted line), using arbitrary units. As expected, $M \to m$ for $|q| \gg L$. However, in the neighborhood of the barrier there is a small increase of the mass. In contrast, inside the barrier the mass is lowered. For larger quantum effects, we observe a displacement of the location of the mass peak, as well as an increase of the mass peak.

In Fig. 2, we consider the potential V^Q for $m=1$, $L=1/2$, $V_0=1$, $\beta=1/8$, $\varepsilon=\frac{1}{4}$ and for varying $\hbar$. For $\hbar=0$, the classical square barrier is recovered. For larger quantum effects ($\hbar=3$ for the dashed line and $\hbar=6$ for the dotted line), we see

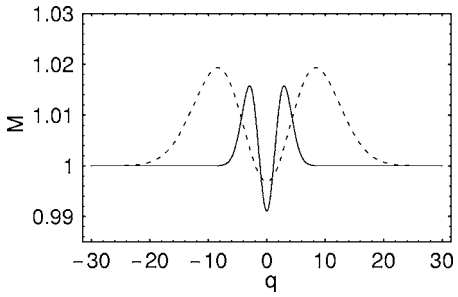

FIG. 1. Space-dependent mass with $m=1$, $L=1/2$, $V_0=1$, $\beta=1/8$, and two different values of $\hbar$, namely, $\hbar=10$ (full line) and $\hbar=30$ (dotted line), using arbitrary units.

an increasing smoothing of the potential V^Q. The height of V^Q becomes smaller for larger quantum effects, increasing tunneling. The observed smoothing is somewhat reminiscent of the smearing of the self-consistent hole potential for quantum plasmas described by the Wigner-Poisson system.[10] In spite of the small increase of the mass $M(q)$ near the barrier, the net result of the effective quantum potential is clearly the lowering of the barrier. Similar smoothing effects were also observed for other effective quantum potential theories.[11]

To obtain a condition for tunneling, consider that, for not too big quantum effects, the maximum of V^Q is obtained for $q=0$. For very large quantum effects, we can show graphically that the maximum of V^Q is not at $q=0$ anymore, being displaced to symmetric positions around the origin. However, in these cases the smoothing is very strong. Disregarding this possibility, we obtain the analytical expression

$$\max(V^Q) = V^Q(0) = \left[1 + \frac{2V_0L}{3\hbar}\left(\frac{2\beta m}{\pi}\right)^{1/2}\exp\left(-\frac{2mL^2}{\beta\hbar^2}\right)\right] \times \left[V_0\operatorname{erf}\left(\frac{\sqrt{2m}L}{\sqrt{\beta\hbar^2}}\right) - \varepsilon\right] + \varepsilon. \tag{19}$$

For a classical particle of energy ε to surpass the barrier V^Q, it is necessary that $\varepsilon > \max(V^Q)$. With (19), this gives

$$\varepsilon > V_0\operatorname{erf}\left(\frac{\sqrt{2m}L}{\sqrt{\beta\hbar^2}}\right), \tag{20}$$

the tunneling condition in our classical description. For $\hbar \to 0$ it reduces simply to $\varepsilon > V_0$ as expected. Also, tunneling

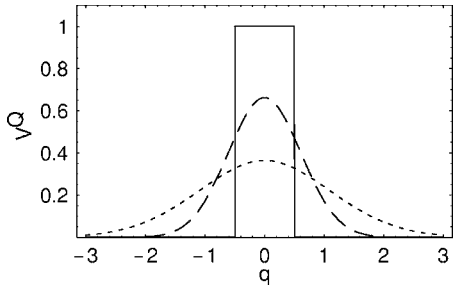

FIG. 2. The potential V^Q for $m=1$, $L=1/2$, $V_0=1$, $\beta=1/8$, $\varepsilon=1/4$ and $\hbar=0$ (full line), $\hbar=3$ (dashed line), and $\hbar=6$ (dotted line). We consider arbitrary units.

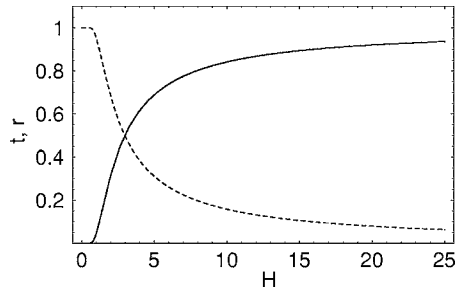

FIG. 3. Transmission coefficient t (full line) and reflection coefficient r (dotted line) as functions of the nondimensional parameter $H=\sqrt{\beta/m}\hbar/L$ in the case of an homogeneous incoming beam.

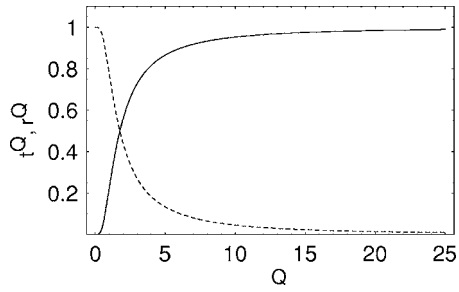

FIG. 4. Transmission coefficient t^Q (full line) and reflection coefficient r^Q (dotted line) as functions of the nondimensional parameter $Q=\hbar/(\sqrt{mV_0}L)$ in the case of an homogeneous incoming beam.

is increased for small temperatures and for a small thickness of the barrier.

As said before, in the present classical model for a quantum process the word "tunneling" is to be used with caution. However, we can even assign an effective "transmission coefficient" to be calculated with the smeared out potential V^Q. Indeed, let a beam of classical particles going from the left against the barrier V^C. Suppose that the beam is constituted by particles with energies ranging from 0 to V_0, with a homogeneous distribution in energy. In other words, the probability $\rho(E)$ to find a particle with energy from 0 to V_0 in a range δE is simply $\rho(E)=\delta E/V_0$. Classically, none of the particles of this hypothetical beam would surpass the barrier. However, if we admit the model of the effective quantum potential (3) and restrict to small energies, so that $\beta V_0 \ll 1$, we can apply the approximation of the preceding sections and define an effective transmission coefficient t given by the ratio of the number of particles that surpass the barrier to those that are reflected. In view of (20), this effective transmission coefficient is

$$t=\frac{V_0-V_0\,\mathrm{erf}(\sqrt{2m}L/\sqrt{\beta\hbar^2})}{V_0}=1-\mathrm{erf}\left(\frac{\sqrt{2m}L}{\sqrt{\beta\hbar^2}}\right). \quad (21)$$

Similarly, we obtain an effective reflection coefficient given by

$$r=\mathrm{erf}\left(\frac{\sqrt{2m}L}{\sqrt{\beta\hbar^2}}\right). \quad (22)$$

Of course we have $t+r=1$. Graphics of t and r are shown in Fig. 3, where once again we see that larger quantum effects increase tunneling. In this particular example, quantum effects are measured by the nondimensional quantity $H=\sqrt{\beta/m}\hbar/L$. Significant tunneling begins to happen for $H\approx 2$. For $H=2.97$ we have already 50% of the particles surpassing the barrier.

We have defined a transmission coefficient well suited for the classical description we have adopted. It is interesting to compare this to a truly quantum description. A quantum version of the preceding situation would be a statistical mixture of incoming eigenstates of well-defined energy $\{\psi(x)=e^{ikx}\}$, where $\psi(x)$ is a particular eigenfunction on the ensemble. Here, we are considering particles going from the left ($k>0$) with an energy $E=\hbar^2k^2/(2m)$. Hence, we have $dE/V_0=\hbar^2kdk/(mV_0)$, so that the probability of finding a state with wave number k in the ensemble would be $\rho(k)=\hbar^2k_0/(mV_0)$, for $0\leqslant k\leqslant k_0$ and zero otherwise, where $k_0=\sqrt{2mV_0}/\hbar$. We have the proper normalization $\int_0^{k_0}\rho(k)dk=1$ as it should be.

What is the "transmission coefficient" associated to this statistical mixture? For just one incoming eigenstate e^{ikx}, any textbook on quantum mechanics gives the result

$$t^Q_{\mathrm{one}}=\frac{k^2(k^2-k_0^2)}{k^4-k_0^2k^2-(k_0^4/4)\sinh^2(2\sqrt{k_0^2-k^2}L)} \quad (23)$$

for this transmission coefficient. For the statistical mixture just described, due to the linearity of the Schrödinger equation the transmission coefficient is given by the average

$$t^Q=\int_0^\infty t_{\mathrm{one}}(k)\rho(k)dk, \quad (24)$$

or, after some easy scalings and rearrangements,

$$t^Q=2\int_0^1\frac{x^3(x^2-1)dx}{x^4-x^2-(1/4)\sinh^2(2\sqrt{1-x^2}/Q)}. \quad (25)$$

In (25) the quantum transmission coefficient is a function of the parameter $Q=(k_0L)^{-1}=\hbar/(\sqrt{mV_0}L)$ only, whereas the parameter $H=\sqrt{\beta/m}\hbar/L$ is present in the effective quantum potential description. In Fig. 4 we show the quantum transmission coefficient t^Q as well as the quantum reflection coefficient $r^Q=1-t^Q$ as functions of Q. For $Q=1.75$ we have already $t^Q=0.5$. As seen comparing Figs. 3 and 4, the transmission coefficients for the effective quantum potential and quantum statistical mixture problem have similar functional behaviors in spite of the somewhat different analytical expressions (21) and (25) and the different relevant quantum parameters H and Q. In a sense, this supports the viewpoint that V^Q adequately simulates tunneling, even in our low-momentum approximation.

In more realistic laboratory conditions, usually one has not an incoming beam with an homogeneous probability distribution in energy as in the previous calculations. Instead, more often we have an incoming beam described by a Gaussian probability distribution. To be specific, consider a normal distribution centered at $p_0/2$, where $p_0=(2mV_0)^{1/2}$ is the minimum momentum for passing particles in the purely classical case. In addition, let the variance be δp^2. In this case,

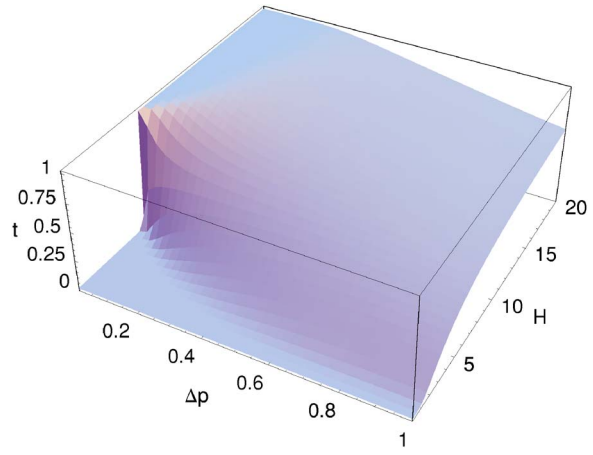

FIG. 5. Transmission coefficient t as functions of the nondimensional parameters $H=\sqrt{\beta/m\hbar}/L$ and $\Delta p=2\sqrt{2}\delta p/p_0$ in the case of a Gaussian incoming beam.

we would have an incoming beam whose probability distribution in momentum is

$$\rho(p)=\frac{1}{\sqrt{2\pi}\delta p}\exp\left[-\frac{(p-p_0/2)^2}{2\delta p^2}\right]. \tag{26}$$

Proceeding as before, we obtain a classical transmission coefficient given by

$$t=\int_{p_0^*}^{p_0}\rho(p)dp, \tag{27}$$

where

$$p_0^*=p_0[\mathrm{erf}(\sqrt{2}/H)]^{1/2} \tag{28}$$

is the momentum threshold for the smoothed potential, as follows from (20). Performing the integration, the result is

$$t=\frac{1}{2}\left[\mathrm{erf}\left(\frac{1}{\Delta p}\right)+\mathrm{erf}\left(\frac{1}{\Delta p}(1-2[\mathrm{erf}(\sqrt{2}/H)])^{1/2}\right)\right], \tag{29}$$

where $\Delta p=2\sqrt{2}\delta p/p_0$. We can also define an effective reflection coefficient $r=1-t$. Graphics for the effective transmission coefficient is shown in Fig. 5 for H ranging from 0 to 20 and Δp ranging from 0 to 1. For small momentum dispersion, that is, for small Δp, we observe a sudden jump in the transmission coefficient. This can be explained in the following way. For small momentum dispersion, the incoming beam is constituted almost only by particles with momentum $p_0/2$. The condition for tunneling in this case traduces into $p_0/2>p_0^*$. Using (28), this gives an inequality for H. Numerically solving, this yields $H>6.28$, the condition for tunneling in the classical picture for small momentum dispersion. In Fig. 6, the effective transmission coefficient for a Gaussian beam centered at $p_0/2$ is shown taking $\Delta p=0.005$. A jump around $H=6.28$ is indeed clearly seen. For larger Δp, the sudden jump disappear as apparent in Fig. 5.

Other relevant results from the effective transmission coefficient (29) can also be collected,

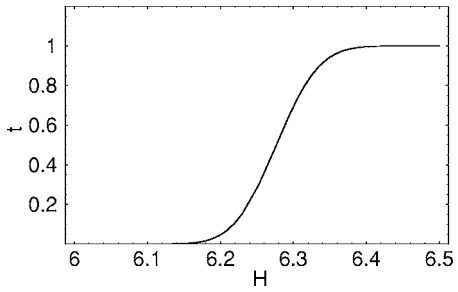

FIG. 6. Sudden jump in the transmission coefficient t as functions of the nondimensional parameters $H=\sqrt{\beta/m\hbar}/L$, for $\Delta p=0.005$ in the case of a Gaussian incoming beam.

$$\lim_{H\to 0} t=0,\quad \lim_{H\to\infty} t=\mathrm{erf}(1/\Delta p),\quad \lim_{\Delta p\to\infty} t=0. \tag{30}$$

The first result at (30) simply says that for no quantum effects there are no tunneling particles. The second result shows that the probability of *quantum* tunneling decreases for increasing momentum dispersion, even for very large H. The reason for this is that for large momentum dispersion there is a significant fraction of particles with momentum greater than the classical threshold p_0. Hence, the transport of particles across the square barrier would have no relation with quantum effects. In fact, for greater Δp a smaller value of the effective transmission coefficient for large H is seen in Fig. 5. Finally, the last result at (30) can be also understood in terms of an increasing probability of purely classical transport across the barrier, for increasing momentum dispersion.

There are at least two possible quantum versions of the classical Gaussian beam just considered. One, more traditional, possibility is to take as initial condition a Gaussian wave packet going from the left and then to solve the time-dependent Schrödinger equation to obtain the asymptotic state. This is a classical problem for which the exact solution was recently found in terms of elementary functions.[12] However, the results of this avenue are not so easily comparable to the present approach. Instead, we consider a statistical mixture of incoming eigenstates of well-defined energy $\{\psi(x)=e^{ikx}\}$, with a Gaussian probability distribution in wave numbers,

$$\rho(k)=\frac{\hbar}{\sqrt{2\pi}\delta p}\exp\left[-\frac{(\hbar k-p_0/2)^2}{2\delta p^2}\right]. \tag{31}$$

The detailed study of the time evolution of a Gaussian wave packet is certainly useful, but for our purposes (restricted essentially to the asymptotic states), this statistical mixture picture is sufficient. In addition, analytical results are more easily derivable. Indeed, for the quantum transmission coefficient t^Q we use again (24) restricting to the range $0\leqslant k\leqslant p_0/\hbar$ and a momentum distribution $\rho(k)$ now given by (31). The result is

$$t^Q=\frac{2}{\sqrt{\pi}\Delta p}\int_0^1\exp\left[\frac{-4(x-1/2)^2}{\Delta p^2}\right]\times\left[\frac{x^2(x^2-1)dx}{x^4-x^2-(1/4)\sinh^2(2\sqrt{1-x^2}/Q)}\right], \tag{32}$$

where $\Delta p=2\sqrt{2}\delta p/p_0$ and $Q=\hbar/(p_0L)$ as before. In Fig. 7

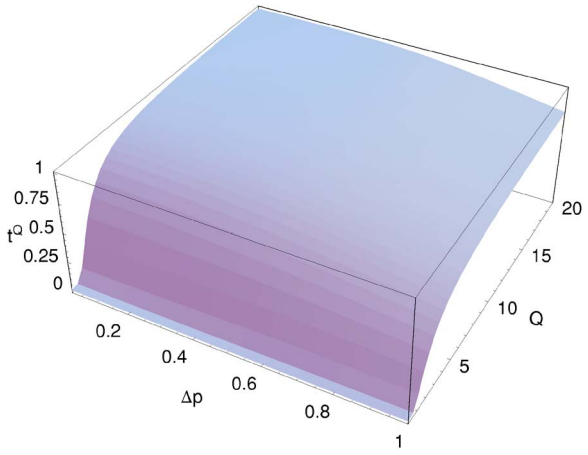

FIG. 7. Transmission coefficient t^Q as functions of the nondimensional parameters $Q=\hbar/(\sqrt{mV_0}L)$ and $\Delta p=2\sqrt{2}\delta p/p_0$ in the case of a Gaussian incoming beam.

we show t^Q for for H ranging from 0 to 20 and Δp ranging from 0 to 1. In contrast to the effective potential picture, we observe no sudden jump of the quantum transmission coefficient. This is related to the different nature of the particle transport, in the effective quantum potential theory and in the true quantum statistical mixture case. In addition, the relevant quantum parameters H and Q are still different, as in the case of the incoming beam with a probability distribution homogeneous in energy. However, for moderate momentum dispersion we observe similarities between the transmission coefficients t at Fig. 5 and t^Q at Fig. 7, even if the quantum parameters H and L have different expressions.

To conclude this section, we collect some extra results, to be compared with (30),

$$\lim_{H\to 0} t^Q = 0, \quad \lim_{H\to\infty} t^Q = \mathrm{erf}(1/\Delta p), \quad \lim_{\Delta p\to\infty} t^Q = 0. \quad (33)$$

Other examples (double square barriers, other classical potential forms) can be easily constructed, with results similar to those of this section.

V. CONCLUSION

In this work, the effective quantum potential (3) was studied in a low-energy region of phase space, characterized by $\beta p^2/m \ll 1$. In its original form, the effective quantum potential is a complicated function of momentum. In the low-momentum approximation, we identified a space-dependent mass and a smoothed potential, both obtainable from the classical potential. For one-dimensional problems, the dynamics of a particle with space-dependent mass under a time-independent potential is completely integrable, a fact that allows for a number of conclusions. In particular, we have found the potential V^Q at Eq. (15), which, in the low-momentum approximation, describes the classical motion under the effective quantum potential. In connection to the problem of a square barrier, we proposed effective transmission and reflection coefficients for effective quantum potentials, which were explicitly found with the aid of the exact solution for the equation of motion. Comparison to true quantum transmission and reflection coefficients is allowed if an appropriated quantum statistical mixture is introduced. In the case of a square barrier, we identified two nondimensional parameters measuring the relevance of quantum effects for tunneling, $H=\sqrt{\beta/m\hbar/L}$ for the effective quantum potential model and $Q=\hbar/(\sqrt{mV_0}L)$ for the quantum statistical mixture, besides the momentum variance in the case of a Gaussian incoming beam. Note that both H and Q are increasing functions of $\hbar$ and decreasing functions of the barrier thickness $2L$. These features are consistent from what one would expect from quantum tunneling processes.

In conclusion, we have obtained a more detailed physical interpretation of the effective quantum potential (3), in terms of a space-dependent mass and a smoothed potential, in a low-momentum approximation. We observe both similarities (similar functional behavior) and differences (relevant parameters, a sudden jump in the transmission coefficient for small momentum dispersion) between the effective quantum potential theory and the appropriated quantum statistical mixture. It would be interesting to generalize the results of this work to more dimensions. In particular, it would be interesting to investigate the integrability of potentials V^Q obtained from higher-dimensional integrable classical potentials.

ACKNOWLEDGMENTS

We thank the Brazilian agency Conselho Nacional de Desenvolvimento Cien tífico e Tecnólogico (CNPq) for financial support.

*Email address: ferhaas@exatas.unisinos.br

[1] P. A. Markowich, C. Ringhofer, and C. Schmeiser, *Semiconductor Equations* (Springer-Verlag, New York, 1990).
[2] F. Haas, G. Manfredi, and J. Goedert, Phys. Rev. E **64**, 026413 (2001).
[3] R. P. Feynman and H. Kleinert, Phys. Rev. A **34**, 5080 (1986).
[4] D. K. Ferry, S. Ramey, L. Shifren, and R. Akis, J. Comput. Electron. **1**, 59 (2002).
[5] C. Ringhofer, C. Gardner, and D. Vasileska, Int. J. High Speed Electron. Syst. **13**, 771 (2003).
[6] S. Ahmed, C. Ringhofer, and D. Vasileska, J. Comput. Electron. **2**, 113 (2003).
[7] S. Ahmed, C. Ringhofer, and D. Vasileska, Superlattices Microstruct. **34**, 311 (2004).
[8] L. Shifren, L. R. Akis, and D. K. Ferry, Phys. Lett. A **274**, 75 (2000).
[9] D. K. Ferry and J.-R. Zhou, Phys. Rev. B **48**, 7944 (1993).
[10] A. Luque, H. Schamel, and R. Fedele, Phys. Lett. A **324**, 185 (2004).
[11] R. Giachetti and V. Tognetti, Phys. Rev. B **33**, 7647 (1986).
[12] A. L. P. Prieto and S. Brouard, J. Phys. A **36**, 2371 (2003).